Accepted Author Manuscript: N. Kumar et al, Appl. Phys. Lett. 111, 213502 (2017)

A tapered multi-gap multi-aperture pseudospark-sourced electron gun based X-band slow wave oscillator

N. Kumar[1], R. P. Lamba[1], A. M. Hossain[1], U. N. Pal[1], A. D. R. Phelps[2] and R. Prakash[1]

[1]*CSIR-CEERI, Pilani-333031, Rajasthan, India*

[2]*Department of Physics, SUPA, University of Strathclyde, Glasgow G4 0NG, United Kingdom*

Abstract

The experimental study of a tapered, multi-gap, multi-aperture pseudospark-sourced electron gun based X-band plasma assisted slow wave oscillator is presented. The designed electron gun is based on the pseudospark discharge concept and has been used to generate a high current density and high energy electron beam, simultaneously. The distribution of apertures has been arranged such that the field penetration potency inside the backspace of the hollow-cathode is different while passing through the tapered gap region. This leads to non-concurrent ignition of the discharge through all the channels that is, in general, quite challenging in the case of multi-aperture plasma cathode electron gun geometries. Multiple and successive hollow cathode phases are reported from this electron gun geometry, which have been confirmed using simulations. This geometry also has led to the achievement of ~71 % fill factor inside the slow wave oscillator for an electron beam of energy 20 keV and beam current density 115-190 A/cm^2 at a working argon gas pressure of 18 Pa. The oscillator has generated broadband microwave output in the frequency range 10-11.7 GHz with a peak power of ~10 kW for ~50 ns.

Plasma assisted slow wave oscillators are potential candidates for applications that include directed energy sources, decoys and noise generators for jamming, where particularly in airborne applications ~~where~~ size and weight reductions are important.[1,2] The power handling capabilities of vacuum microwave sources especially falls because of the miniaturized RF structures in the millimeter and sub-millimeter wave regions.[3,4] To overcome this problem, the possibility of using a plasma-filled interaction structure in which electrons can propagate far enough from the metallic walls is very attractive.[1-3] The available literature reveals that the presence of a controlled amount of ionized gas (plasma) inside the microwave devices can significantly improve their characteristics beyond what is currently available in evacuated devices.[1,4]

There are basically two broad classifications of plasma filled microwave tubes based respectively on differential pressure based plasma cathode electron guns and pseudospark (PS) based electron guns, each of which have their own advantages and limitations.[1-4] The advantage of the former electron gun is the possibility of generating long pulse energetic electron beams using an active pumping system for evacuating gas from the accelerator region. No such arrangement is essential in pseudospark gun sources, albeit there is a restriction to shorter duration pulses of the generated electron beam. It is very difficult to use the former gun source for those applications where compact low weight systems are required. The shorter pulses of the PS based gun source can be mitigated by operating at higher pulse repetition frequency (PRF) of more than 100 Hz which would mainly depend on the pulse duration of the generated electron beam and the recovery time of the electron gun. The PS based plasma electron beam generation has several advantages when it is used as the electron beam source in plasma assisted microwave tubes.[4-6] The PS based electron beam does not require any applied magnetic field due to the presence of plasma inside the slow wave structure (SWS) during its propagation.[7-8] Moreover, the presence of plasma inside the SWS shifts the beam space charge fields near to the microwave fields.[2] However, to enhance the coupling coefficient between beam space charge and RF fields, the fill factor and current density[9], as well as the energy of the PS based electron beam should be high enough, which critically depends on the geometrical parameters. In recent studies, it has been shown that with a single-gap structure of PS based hollow cathode discharge, the energy of the generated electron beam is lower for multi-aperture as well as single aperture operation.[10,11] Nevertheless, for the multi-gap structure of a PS based hollow cathode discharge, the energy of the generated electron beam is higher but with low current density and also low fill factor. So far there exists no PS based electron beam source that meets the important requirements of simultaneous generation of an electron beam with higher energy, high current density as well as high fill factor to mitigate the issue.

In this letter, we present the results of a designed and developed tapered, multi-gap, multi-aperture (TMGMA) PS based electron beam source to generate X-band microwave radiation. This source has a cascaded tapered-gap region between the hollow cathode and the anode disc, and also

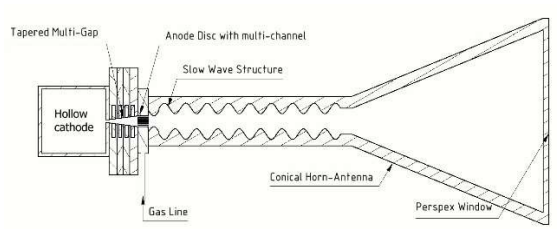

FIG. 1(a). 2D schematic view of X-band slow wave oscillator

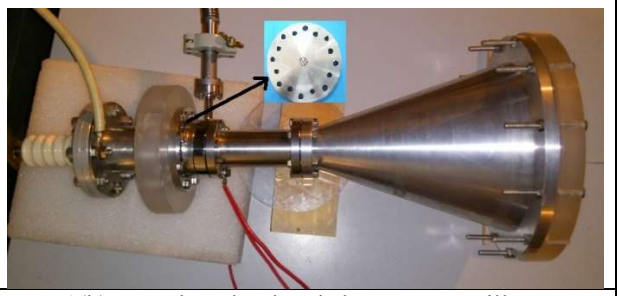

FIG. 1(b). Developed X-band slow wave oscillator

multiple aperture channels developed on the surface of the anode disc.

A schematic and a photograph of the X-band slow wave oscillator consisting of the TMGMA PS based electron beam source, a SWS and conical horn antenna are shown in Figs. 1(a) and Fig. 1(b), respectively. In this TMGMA PS based electron beam source, the cascaded structures of 4 floating anodes and 5 insulators along with optimized tapering have been used. This cascaded structure is placed in between the hollow cathode and anode disc arrangement with proper vacuum sealing as shown in Fig.1 (a). The hollow cathode has a 3 mm diameter aperture whereas the anode disc has 33 equi-spaced apertures of 1mm diameter each placed within the 10 mm diameter periphery in the anode disc (see insert image in Fig. 1 (b)). The apertures of diameter 1mm are radially distributed with spacing of 1.5 mm between them on three pitch circle diameters (PCDs) apart from central aperture. The spacing between each individual aperture has been kept as 0.5 mm so that there will be a uniform cumulative effect. The strength of the electric field inside the backspace of the hollow cathode region varies with the distance between the anode aperture on three different PCDs and the hollow cathode aperture in the tapered gap region. This can lead to non-concurrent ignition of the discharge through all the channels and enables generation of the electron beam in multiple stages of the hollow cathode phase followed by the conductive phase. In the developed PS based electron beam source, the multiple apertures enable propagation of high beam current due to an increase in perveance and high fill factor (i.e. ~71 %) inside the SWS.

Accordingly the SWS has been taken as a rippled wall cylindrical waveguide having an internal radial profile given by $R(z) = R_0 + h \cos(k_0 z)$, where R_0 = 17 mm is the mean radius, h = 5 mm is the ripple height, z_0 = 10 mm is the corrugation periodicity, $k_0 = 2*pi/z_0$ is the wavenumber and z = 0-90 mm is the axial distance. In order to launch the generated microwave output, a conical horn antenna has been designed and constructed. Since the shape of the SWS is cylindrical, the shape of the antenna is taken as conical. The shape of this antenna can be defined as a hollow pipe of circular cross section, which has been flared to a larger opening. The design parameters have been optimized for maximum dissipation of the spent beam electrons and minimal impact of the spent beam electrons on the Perspex window by measuring the percentage of collision counts. It has been estimated that for a 20 keV beam energy and a maximum 100 A beam current, only ~ 8 % of the electrons may impact on the Perspex window, whereas ~ 92% of the spent beam electrons are dissipated. The optimized design parameters are radius of feed 14.35 mm, length of antenna 235.6 mm, radius aperture 90.9 mm and flare angle 18^0.

Experiments have been performed on the PS based electron beam source. The anode was kept grounded while a negative voltage of 20 kV was applied to the hollow cathode at an argon pressure of 18 Pa. A typical V-I waveform for the developed electron gun is shown in Fig. 2. Multiple hollow cathode phases have been observed, namely hollow cathode phase I (30 A/115 Acm^{-2}/18.5 keV) and hollow cathode phase II (50A/ 190 Acm^{-2}/13 keV). The energy spread observed during the first hollow cathode phase is 18-19 keV while during the second hollow cathode phase it is 12-16 keV. The generated electron beam then propagated inside the SWS. The front edge of the electron beam ionizes the gas and forms the plasma, while the electrons following the beam repel the plasma electrons to form the ion-channel which eliminates the requirement for an applied magnetic field.[5] The propagated electron beam interacts with the slow wave structure and leads to the generation of the microwave signal. The observed real time microwave signal is shown in Fig. 3. The real time signal has been obtained using a microwave detector system consisting of receiving horn antenna, attenuators, adaptors, standard X-band band pass filter, high frequency cables and 13 GHz high bandwidth oscilloscope. The frequency of the generated microwave signal has been obtained using

a Fast Fourier Transform (FFT) and it ranges between 10-11.7 GHz during the multiple hollow cathode phase generation of the electron beam (see Fig. 4). The measured peak power of the generated signal is ~10 kW for ~ 50 ns during the hollow cathode phase. It has been deduced by considering the free space loss of 32 dB, a calibrated attenuator loss of 10 dB and component losses of 3 dB.

The frequency of the generated signal is also influenced by the beam plasma frequency. This frequency shift has been obtained using the beam plasma frequency, which is deduced from the experimental data using the relationship $\omega_{be} = \left(e^2 n_b / \gamma \varepsilon_0 m_e\right)$ where γ is the relativistic factor (γ=1.04 i.e. close to 1 for a 20 kV applied voltage) and n_b is the electron beam number density. Considering the beam plasma frequency and Doppler shift term, the beam dispersion relation becomes,[12,13]

$$\omega = k_z v_z \pm \omega_{be}$$

which leads a shift in the frequency in the range 0.5 GHz to 2.75 GHz and is clearly shown in Fig. 5. The addition of plasma frequency has increased the bandwidth of the developed plasma assisted slow wave oscillator. This wide variation of the beam plasma frequency has made this device unique for the developed PS based TMGMA electron beam source due to its successive hollow cathode phases followed by the conductive phase.

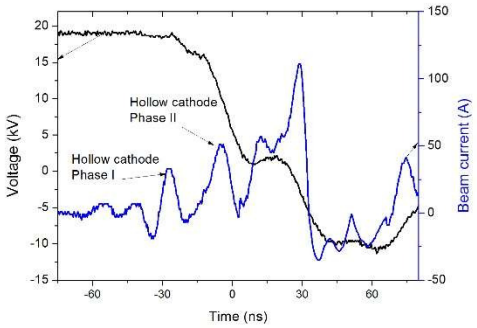

FIG. 2. V-I characteristics of pseudospark based tapered multi-gap multi-aperture electron beam source at ~20 kV applied gap voltage and 18 Pa argon gas pressure

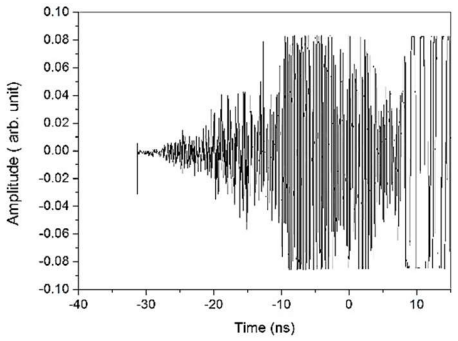

FIG. 3. Real time waveform of the generated microwave signal from X-band slow wave oscillator

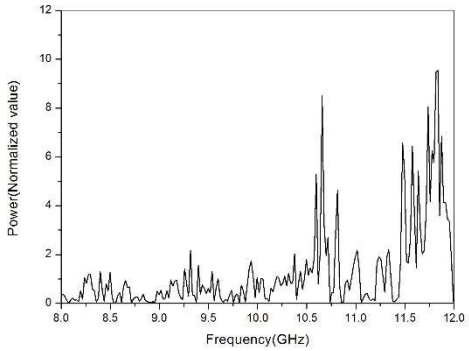

FIG. 4. FFT of generated microwave signal deduced from Fig. 3

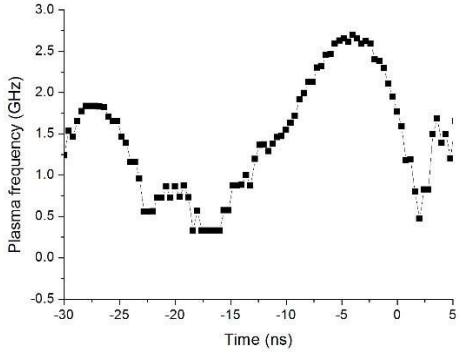

FIG. 5. Beam plasma frequency during multiple hollow cathode phases

To understand this unique feature, simulations have also been performed using the plasma discharge module of the COMSOL 5.2a code. Simulations are carried out on similar geometry to the TMGMA PS based electron beam source for similar operating conditions, i.e., at an argon gas pressure of 18 Pa and an applied potential of 20 kV. The cross-sectional view of the TMGMA PS based electron beam source geometry and anode potential profile is shown in Fig. 6 (a)-(d). Initially at t = 5 ns, the anode

equipotential profile is confined in the tapered region and moves slowly toward the hollow cathode region as shown in Fig. 6 (a). The applied gap voltage drops almost completely in a thin layer of plasma sheath adjacent to the cathode surface as time progresses and is shown in Fig. 6 (b) and 6 (c). This can lead to increase in the electron plasma density (n_e) in the hollow cathode phase because the cathode sheath thickness d_c is dynamic and related to the electron density n_e by the following equation,

$$d_c = \sqrt{2\varepsilon_0 U_c / en_e}$$

where U_c is the voltage drop across the plasma sheath.[12] In the hollow cathode phase, the plasma starts behaving like the anode within a few hundreds of microns from the inner surface of the cathode[14] and it adapts to the cathode morphology as shown in Fig. 6 (c). As the time progresses, it leads to the formation of a virtual anode in close proximity that has the same shape as the cathode, and an extremely high electric field is therefore homogeneously distributed over a large area (see Fig. 6 (d)) where the sheath thickness becomes minimal and the conduction phase occurs. This analysis provides an overall field distribution for the TMGMA PS based source where all the apertures on the anode surface are active.

Further simulations have been carried out to analyze the role of the individual apertures on the field distribution and beam generation during the multiple hollow cathode phases. In the simulations the apertures of diameter 1mm are radially distributed with a spacing of 1.5 mm between them on three PCDs encircling the central aperture exactly similar to the developed source. The simulation analysis has been performed for the electrical potential profile when the apertures on individual PCD's are active, as well as when all the apertures on all PCDs including the central aperture are active. The results are shown in Fig. 7, where the strength of the positive field inside the backspace of the hollow cathode region is varying and it shows dependency on the distance between the anode aperture and hollow cathode aperture in the tapered gap region. This further shows field variation at the same time at different PCDs. It leads to non-concurrent ignition of the discharge through all the channels and enables generation of the electron beam in multiple stages of the hollow cathode phase followed by the conductive phase. The results are clearly visible in Fig. 8, which confirms the multiple hollow cathode phases as measured in the experiments (see Fig. 2). In fact, the distances of different channels on the anode disc from the single aperture of the hollow cathode are variable, which leads to a delay in electric potential penetration. This plays a major role in energetic electron beam generation from the anode in the multiple hollow cathode phases before going into the conduction phase.

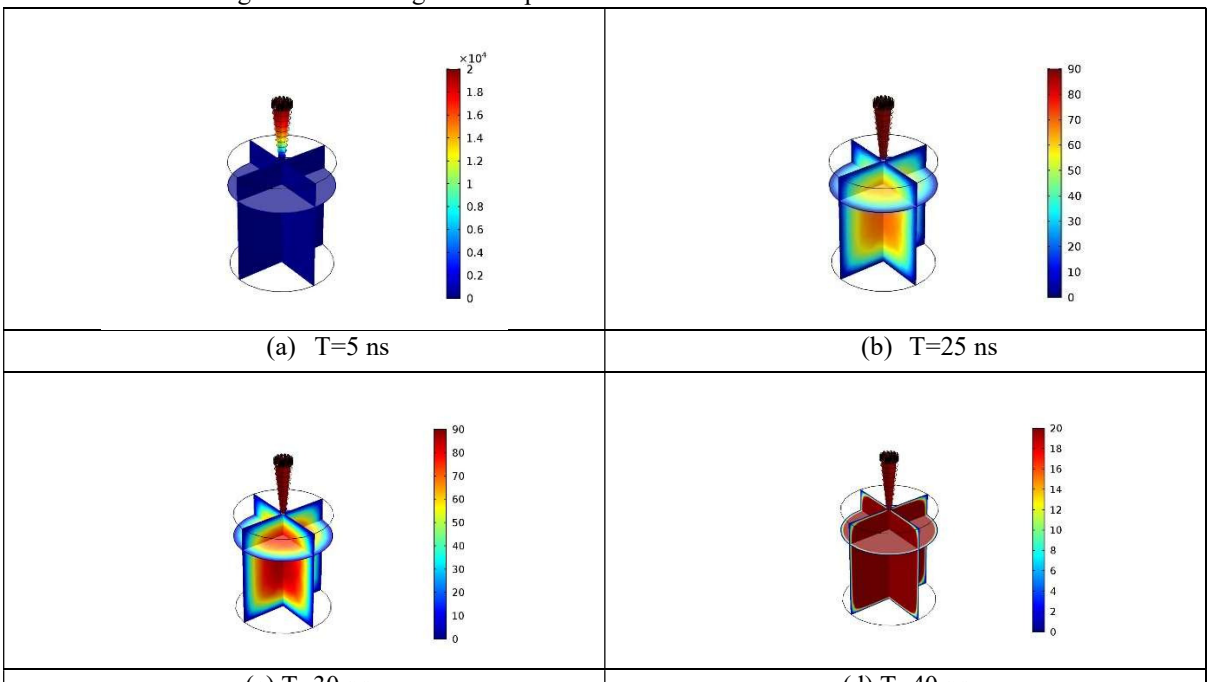

(a) T=5 ns | (b) T=25 ns

(c) T=30 ns | (d) T=40 ns

FIG. 6. Anode potential profiles using simulation at different instants of time

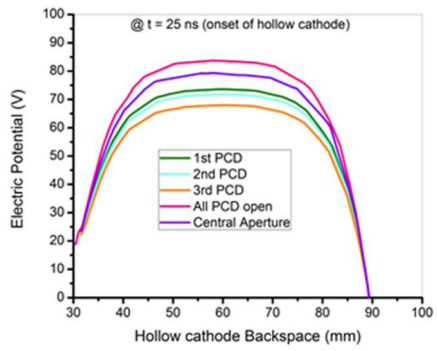

FIG. 7. Electric potential penetration inside the backspace region of the hollow cathode at t=25 ns for 20 kV applied gap voltage and 18 Pa argon gas pressure

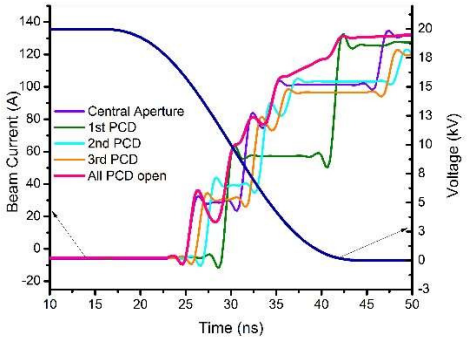

FIG. 8. Simulated V-I characteristics of pseudospark based tapered multi-gap multi-aperture electron beam source at 20 kV applied gap voltage and 18 Pa argon gas pressure

In summary, multiple phases of an energetic electron beam, i.e. during the hollow cathode phase have been generated for the first time by using a ~~novel~~ tapered multi-gap multi-aperture PS based electron beam source. The generation of multiple hollow cathode phases is mainly due to the successive breakdown in the tapered gap region and the non-concurrent ignition of the electron beam by each channel on the anode surface into the interaction region. The developed electron source enables simultaneous generation of high current density, high energy and high fill factor electron beams. A good correlation has been obtained between experimental and numerical simulation results. The observed deviation between the numerical simulation and the measured beam current profile during hollow cathode phase I, hollow cathode phase II and the conduction phase is 6%, 11% and 13%, respectively. This electron beam source has been used for generating microwave signals with peak power 10 kW in the frequency range of 10-11.7 GHz from the developed plasma assisted X-band slow wave oscillator.

[1] M. Botton, Appl. Phys. Lett. **60** (18), 2198 (1992).
[2] D. M. Goebel, Y. Carmel and G. S. Nusinovich, Phys. Plasmas **6**, 2225 (1999).
[3] G. S. Nusinovich, Y. Carmel, A. G. Shkvarunets, J. Rodgers T. M. Antonsen Jr. and V. L. Granatstein, IEEE Trans. Plasma Sci. **52**, 845 (2005).
[4] A.W. Cross, H. Yin, W. He, K. Ronald, A. D. R. Phelps, and L. C. Pitchford, J. Phys. D: Appl. Phys. **40**, 1953 (2007).
[5] H. Yin, A. W. Cross, W. He, A. D. R. Phelps, K. Ronald, D. Bowes, and C. W. Robertson, Phys. Plasmas **16**, 063105 (2009).
[6] G. Liu, W. He, A. W. Cross, H. Yin and D. Bowes, J. Phys. D: Appl. Phys. **46**, 345102 (2013).
[7] G. Shu, W. He, L. Zhang, H. Yin, J. Zhao, A. W. Cross, and A. D. R. Phelps, IEEE Trans. Elect. Dev. **63**, 4955 (2016).
[8] J. Zhao, H. Yin, L. Zhang, G. Shu, W. He, Q. Zhang, A. D. R. Phelps, and A. W. Cross, Phys. Plasmas, **24**, 023105 (2017).
[9] I. V. Konoplev, A. W. Cross, P. MacInnes, W. He, C. G. Whyte, A. D. R. Phelps, C. W. Robertson, K. Ronald, and A. R. Young, Appl. Phys. Lett. **89** (17), 171503 (2006).
[10] N. Kumar, D. Pal, R. P. Lamba, U.N. Pal and R. Prakash, IEEE Trans. Elect. Dev. **64**, 2688 (2017).
[11] N. Kumar, D. K. Pal, A. S. Jadon, U.N. Pal, H. Rahaman and R. Prakash, Rev. Sci. Instr. **87**, 033503 (2016).
[12] W. He, L. Zhang, D. Bowes, H. Yin, K. Ronald, A. D. R. Phelps, and A. W. Cross, Appl. Phys. Lett. **107**, 133501 (2015).
[13] Liu Shenggang, Y. Yang, M. Jie, and D. M. Manos, Phys. Rev. E. **65**, 036411 (2002).
[14] A. Anders, S. Anders and M. A. Gundersen, Phys. Rev. Lett. **71**, 364 (1993).